Research Article

Fahad Alsharari*, Roz-Ud-Din Nassar, Talal O. Alshammari, Md. Alhaz Uddin, and Siyab Ul Arifeen*

Analyzing the viability of agro-waste for sustainable concrete: Expression-based formulation and validation of predictive models for strength performance

https://doi.org/10.1515/rams-2025-0163
received July 28, 2025; accepted September 16, 2025

Abstract: By lowering environmental impact and increasing resource efficiency, agro-waste in concrete provides a sustainable substitute for traditional materials. This study focuses on optimizing concrete mix designs using agricultural byproducts such as corn cob ash, palm oil fuel ash, rice husk ash, sugarcane bagasse ash, and wheat straw ash, alongside water-cement ratio and curing duration. An experimental dataset was compiled, targeting compressive strength (CS) and tensile strength (TS) as output parameters. Two advanced machine learning (ML) techniques, gene expression programming (GEP) and multi expression programming (MEP), were applied for predictive modeling and optimization. Model accuracy was assessed using statistical metrics and Taylor's plots, while SHapley Additive exPlanations analysis was used to interpret input parameter influence. Results showed that MEP outperformed GEP in both CS and TS predictions. For CS, the MEP model achieved an R^2 of 0.963 compared to 0.934 for the GEP model, while for TS, the MEP model reached 0.961 compared to 0.945 for GEP. The study highlights the role of ML in enhancing mix design efficiency, reducing trial-and-error experimentation, and accelerating the development of sustainable, high-performance construction materials. Such studies demonstrate how ML can streamline concrete mix design by minimizing experimental trials, saving both time and resources. By incorporating agro-waste materials, they provide engineers with practical tools to develop sustainable, high-performance concretes that lower environmental impact while maintaining structural reliability.

Keywords: agricultural waste-based concrete, gene and multi expression programming, compressive and tensile strength

*** Corresponding author: Fahad Alsharari,** Civil Engineering Department, Jouf University, Sakaka, Jouf, 72388, Saudi Arabia, e-mail: fdralsharari@ju.edu.sa
*** Corresponding author: Siyab Ul Arifeen,** Department of Civil Engineering, COMSATS University Islamabad, Abbottabad, 22060, Pakistan, e-mail: engrsiyabularifeen@outlook.om
Roz-Ud-Din Nassar: Department of Architecture and Civil Engineering, American University of Ras Al Khaimah, Ras Al Khaimah, United Arab Emirates
Talal O. Alshammari, Md. Alhaz Uddin: Civil Engineering Department, Jouf University, Sakaka, Jouf, 72388, Saudi Arabia

1 Introduction

Due to its significant use as a critical building material, the environmental impact of concrete has been thoroughly examined over many years [1]. Cement and concrete demand is projected to triple by 2050, leading to faster-than-expected increases in carbon emissions and reductions in ecosystem diversity [2]. Researchers are looking for alternative materials with lower carbon footprints [2,3]. Binding concrete requires Portland cement, whose production utilizes around 1.80 metric tons of raw materials and produces about 0.8 metric tons of carbon dioxide gas [4]. Consequently, immediate action is required to decrease cement output in order to diminish the environmental impact [2]. One methodical and technical approach to ensure the materials' long-term viability is recycling waste from agriculture and industry into new construction materials [5,6]. Production of supplementary cementitious materials (SCMs) from recycled materials from agriculture and manufacturing has societal, economic, and ecological advantages [7–9]. Substituting recycled materials for Portland cement is an efficient, long-term, and economical approach to reduce environmental impact [10–12].

The materials for this investigation were agro-wastes, which are both common and cheap, because they are sustainable and practical. Statistical analysis in both developed and developing nations shows that biomass only makes up around 9–14% of total energy sources [13]. Major environmental problems might arise from the widespread practice of leaving wastes behind or burning them in fields. In addition to their use as extra cementitious materials, these agro-waste products can also be used as alternative aggregates in building projects [14]. When compared to developing nations, developed nations are usually better at managing and making use of agricultural waste [15]. Simultaneously, emerging nations are highly focused on finding the right ways to tackle environmental and wastage concerns [16,17]. Because of the palm oil industry's significance to Thailand's agro-industries, the country's resource usage of palm oil ash is a major worry [18]. Still, every year, a mountain of solid trash is generated, comprising things like palm fiber remnants, rice husks, sugarcane bagasse, and wheat straw. Not only does the yearly growth in disposal take up a lot of room, but it also produces major issues including air pollution and possible health and safety risks following combustion. The use of agro-waste ash as a cement component, however, has attracted the attention of numerous researchers. Scientific investigations have shown that agro-waste ash has the potential to be utilized as a pozzolanic material due to its high concentration of amorphous silica [19,20]. By partially replacing 10–30% of cement with agro-wastes, researchers have proven the importance of agro-waste ash in producing high-strength concrete [21]. Cement that contains agro-waste ash has shown excellent performance in mortar and concrete, even when exposed to a hydrochloric acid solution [21], despite these substitutions. Research from all across the globe has shown that agro-wastes are essential [22], therefore it is a good idea to compile all the relevant data in one spot before we introduce new kinds of these wastes or think about their potential future uses.

Researchers, computer scientists, engineers, and scientists are realizing that artificial intelligence (AI) is changing product development. The engineering field faces numerous challenges, creating a growing demand for professionals skilled in artificial intelligence. Despite its potential, AI-based systems have limitations and performance issues. Natural conversation understanding and object identification are activities humans take for granted, but AI algorithms struggle with them [23]. In order to solve these issues, AI systems have used machine learning (ML) [23–25]. Computers can learn to operate independently with the help of ML algorithms by studying large enough datasets [26,27]. Returning to the features that produce the most explicit data is crucial prior to implementing the plan. To explain this process, the word "feature extraction" is now utilized. After that, pattern separation instructions, characteristics, and sample data are trained using ML [23,28,29]. Studies in civil engineering nowadays use statistical methods and AI to tackle challenges that are progressively more complex. Compressive strength (CS) estimation is one area where civil engineers utilize AI and statistical methodologies [30,31]. By applying these methods, several major obstacles were overcome. These included self-compacting concrete slump and impact strength forecasts, structural beam shear behavior, and chloride contamination risk [32–35]. Future research can save time and money by using improved prediction methods. Many ML algorithms seem to promise concrete strength estimation. Extreme Gradient Boosting, multi expression programming (MEP), Decision Trees, Gaussian Process Regression, expression trees (ETs), and gene expression programming (GEP) are examples. These data-centric approaches provide accurate, efficient material property evaluation without traditional testing [36–39]. The mechanical properties of agro-waste-derived concrete were more accurately predicted by symbolic regression-based models, such as GEP and MEP, compared to other ML techniques, owing to their ability to evolve explicit mathematical relationships and capture complex nonlinear patterns in the data.

To reliably predict the CS and tensile strength (TS) of concrete made from agro-waste, a reliable computing framework can be constructed with the help of ML algorithms that have been properly trained. This research utilizes openly accessible experimental datasets to develop predictive regression models aimed at estimating the CS and TS of concrete incorporating agro-waste materials, employing GEP and MEP techniques. There are 700 data points in the collection, drawn from the most recent research on CS and TS. Model validation was accomplished using statistical tests and analysis of Taylor's diagrams. A SHapley Additive exPlanations (SHAP) analysis and sensitivity research were performed to further investigate the effects of different parameters on our predictions. The construction industry stands to benefit greatly from advanced data-driven methods, such as ML models, that can accurately evaluate and predict material properties with minimal human intervention. In the context of this study, such approaches not only reduce reliance on extensive trial-and-error testing but also enable the effective utilization of agro-waste materials, promoting sustainability and innovation in concrete production.

2 Framework of the study

2.1 Dataset assembling and review

This work employed MEP and GEP approaches to anticipate the CS and TS of agro-waste derived concrete, respectively. A total of 700 data points were collected through experimental investigations, comprising values for both CS and TS [40–59]. This study employed seven variables to foresee CS and TS, such as corn cob ash content (CCA), palm oil fuel ash content (POA), rice husk ash content (RHA), sugarcane bagasse ash content (SBA), wheat straw ash content (WSA), water to cement ratio (WCR), and curing duration (CD). Thorough data preparation was crucial for the data collection and organization processes. An effective approach for overcoming a significant challenge is to prepare data for data mining; this fits in with the widely-used knowledge discovery from data methods. To simplify and improve the data, preparation primarily aims to remove distortion and unnecessary portions. Several descriptive statistics were calculated using these data and their results are displayed in Table 1. As an initial stage in ML investigations, descriptive statistics help us comprehend the distribution, central tendency, and variability of the input material. There are a total of 700 samples in the dataset, broken down as follows: CCA, POA, RHA, SBA, and WSA, as well as WCR, CD, and the desired outcomes CS and TS. With a mean WCR of around 0.54 and an average curing day of about 39, the data show moderate amounts of cementitious replacements. The input variables, particularly the percentages of SCMs and the CD, show a great deal of variability, as seen by the standard deviations and ranges. This variability may impact the generalizability of the model. A strong right-tailed distribution is shown by the high kurtosis and skewness values of SCMs. The clustering of most values near 0 indicates that many mixes did not have partial replacements. The construction and validation of accurate ML models depend on a thorough understanding of data behavior, which can be achieved through statistical profiling.

Figure 1(a) and (b) illustrate the Pearson correlation matrices for the datasets associated with CS and TS, respectively. These visualizations depict the linear relationships among the input variables and their corresponding strength outputs, using color-coded ellipses and numerical correlation values (ranging from −1 to +1). The red ellipses indicate positive correlations, while blue signifies negative relationships; the intensity and shape reflect the correlation magnitude. In Figure 1(a) and (b), moderate positive correlations can be seen between CD and both strength properties (CS and TS), with correlation coefficients nearing +0.25. This indicates that longer CDs generally contribute positively to strength development. WCR shows a weak but negative correlation with strength, consistent with established concrete behavior. In contrast, the five SCMs (CCA, POA, RHA, SBA, WSA) exhibit slight negative correlations with the outputs, suggesting that excessive replacement may reduce strength in some mixes. Similar patterns are observed in Figure 1(b) for the TS dataset, although minor variations in correlation values suggest differing sensitivity of compressive and TSs to certain input variables. It is important to note that low correlation values near zero do not necessarily imply independence; nonlinear effects or complex interactions may still exist. Therefore, additional interpretative tools such as SHAP values or sensitivity analysis are recommended to gain a more comprehensive understanding of input–output relationships in predictive modeling.

2.2 ML framework

The CS and TS of agro-waste-based concrete were predicted using a dataset curated through an extensive analysis of prior research studies. Seven input features were considered essential for estimating the corresponding CS and TS values. GEP and MEP, recognized as high-performing ML methods, were employed to develop the predictive models. Typically, ML model accuracy is evaluated by comparing output predictions to actual recorded values. In this study, the dataset was split into two segments, 70% was allotted for training the models,

Table 1: Descriptive overview of ML dataset features

Metrics	CCA (%)	POA (%)	RHA (%)	SBA (%)	WSA (%)	WCR	CD (Days)	CS (MPa)	TS (MPa)
Mean	6.003	5.105	6.014	4.320	5.086	0.540	38.690	44.417	3.990
Standard error	0.491	0.464	0.485	0.428	0.459	0.004	1.240	0.377	0.063
Median	0.000	0.000	0.000	0.000	0.000	0.542	28.000	44.359	3.919
Mode	0.000	0.000	0.000	0.000	0.000	0.664	28.000	29.023	1.552
Standard deviation	12.981	12.268	12.821	11.329	12.145	0.108	32.795	9.968	1.662
Sample variance	168.505	150.511	164.389	128.344	147.490	0.012	1075.530	99.368	2.762
Kurtosis	3.011	4.342	2.976	6.015	4.019	−1.195	−1.249	−1.285	−1.216
Minimum	0.000	0.000	0.000	0.000	0.000	0.351	3.000	27.895	1.169
Maximum	49.998	49.805	49.883	49.815	49.859	0.719	90.000	61.744	6.782
Count	700.000	700.000	700.000	700.000	700.000	700.000	700.000	700.000	700.000

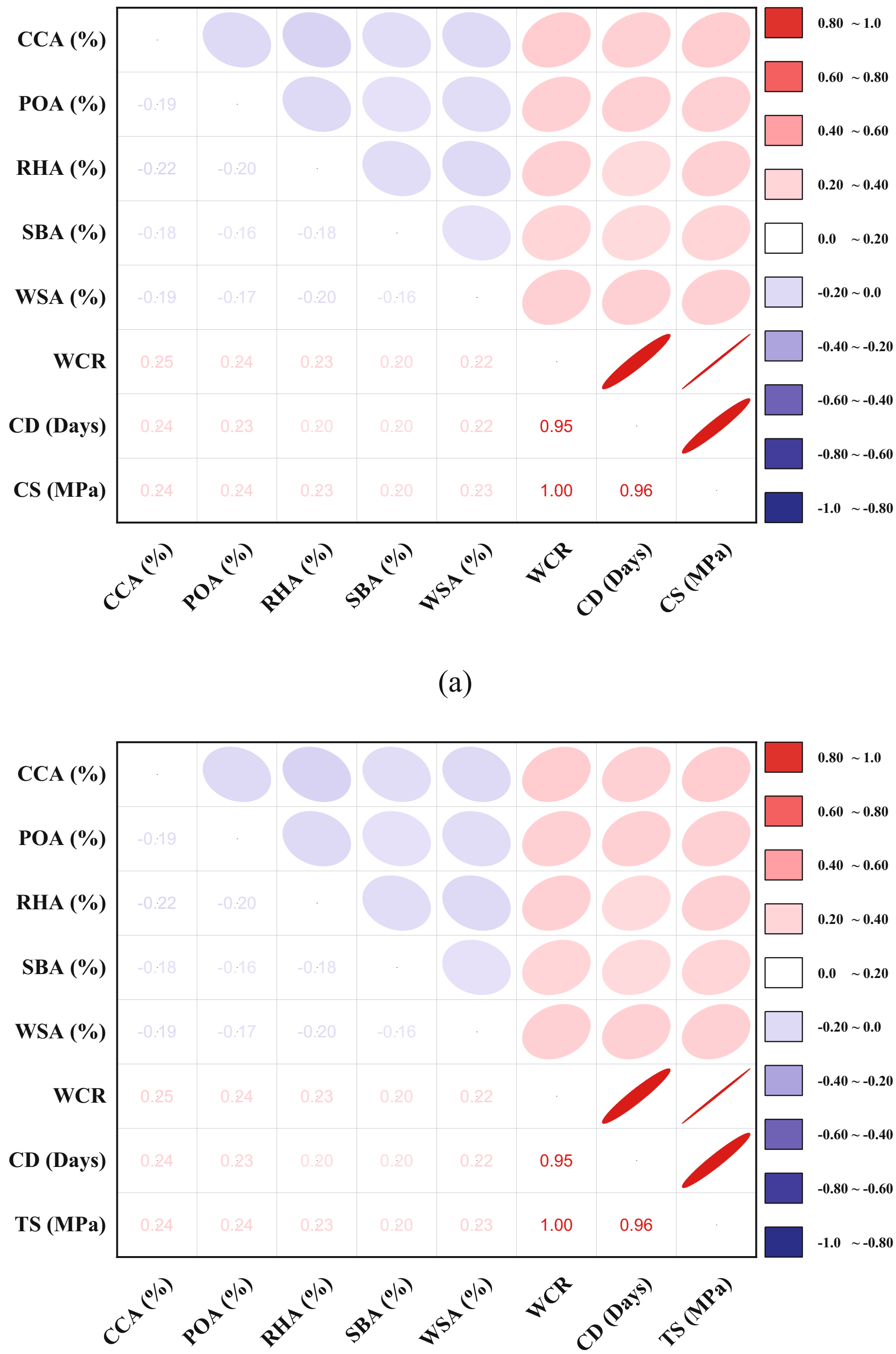

Figure 1: Correlation matrices highlighting key variable interdependencies for (a) CS dataset and (b) TS dataset.

while the rest 30% was utilized to test their generalization performance. The predictive strength of the models was primarily judged by the R^2 score, where a higher value indicates close alignment between estimated and true values, whereas a lower score reveals inconsistencies and reduced reliability [60]. A number of tests, including statistical analyses and evaluations of errors, were conducted to ensure that the model was reliable. Table 2 lists the critical hyperparameters controlling the GEP and MEP models' performance, and Figure 2 shows a scenario-based model representation.

2.3 Performance metrics and accuracy evaluation

The predictive capability of the GEP and MEP models was evaluated on the test dataset using a range of statistical indicators. The assessment incorporated metrics such as root mean square error (RMSE), mean absolute percentage error (MAPE), Nash–Sutcliffe efficiency (NSE), relative root mean square error (RRMSE), mean absolute error (MAE), relative squared error (RSE), and Pearson's correlation coefficient (R), providing a comprehensive measure of the models' accuracy and reliability [61–65]. Eqs. (1)–(7) outline the mathematical expressions used to quantify different statistical indicators that evaluate the predictive performance of the models.

$$R = \frac{\sum_{i=1}^{n}(a_i - \bar{a}_i)(p_i - \bar{p}_i)}{\sqrt{\sum_{i=1}^{n}(a_i - \bar{a}_i)^2 \sum_{i=1}^{n}(p_i - \bar{p}_i)^2}}, \quad (1)$$

$$\mathrm{MAE} = \frac{1}{n}\sum_{i=1}^{n}|p_i - a_i|, \quad (2)$$

$$\mathrm{RMSE} = \sqrt{\sum \frac{(p_i - a_i)^2}{n}}, \quad (3)$$

$$\mathrm{MAPE} = \frac{100\%}{n}\sum_{i=1}^{n}\frac{|p_i - a_i|}{a_i}, \quad (4)$$

$$\mathrm{RSE} = \frac{\sum_{i=1}^{n}(a_i - p_i)^2}{\sum_{i=1}^{n}(\bar{a} - a_i)^2}, \quad (5)$$

$$\mathrm{NSE} = 1 - \frac{\sum_{i=1}^{n}(a_i - p_i)^2}{\sum_{i=1}^{n}(a_i - \bar{p}_i)^2}, \quad (6)$$

$$\mathrm{RRMSE} = \frac{1}{|\bar{a}|}\sqrt{\frac{\sum_{1=1}^{n}(a_i - p_i)^2}{n}}. \quad (7)$$

In this context, n represents the total number of data points, while a_i and p_i correspond to the observed and predicted values for each instance. The symbols $\bar{a}$ and $\bar{p}$ indicate

Table 2: Configured parameters for MEP and GEP models

Category	MEP settings	GEP settings
Data type	Real numbers	Floating number
Problem type	Symbolic regression	Symbolic regression
Function set	+, −, ×, ÷, power, log	+, −, ×, ÷, power, log
Error measure	Mean absolute error	Mean absolute error
Operators/variables	0.5	—
Code length/head size	Code length: 50	Head size: 8
Number of chromosomes	—	30
Number of genes	—	4
Constant per gene	—	10
Linking function	—	Addition
Population structure	2 sub-populations, each with 200 individuals	—
Number of runs	10	—
Number of generations	500	—
Replication number	15	—
Crossover type	Uniform	—
Crossover probability	0.9	—
Mutation probability	0.01	—
Number of threads	2	—
Mutation rate	—	0.00138
Leaf mutation rate	—	0.00546
Stumbling mutation	—	0.00141
Inversion rate	—	0.00546
IS transposition rate	—	0.00546
RIS transposition rate	—	0.00546
Gene transposition rate	—	0.00277
Gene recombination rate	—	0.00277
One-point recombination	—	0.00277
Two-point recombination	—	0.00277
Random chromosomes	—	0.0026
Bounds	Lower: −10, Upper: 10	Lower: −10, Upper: 10
General	CS and TS	CS and TS

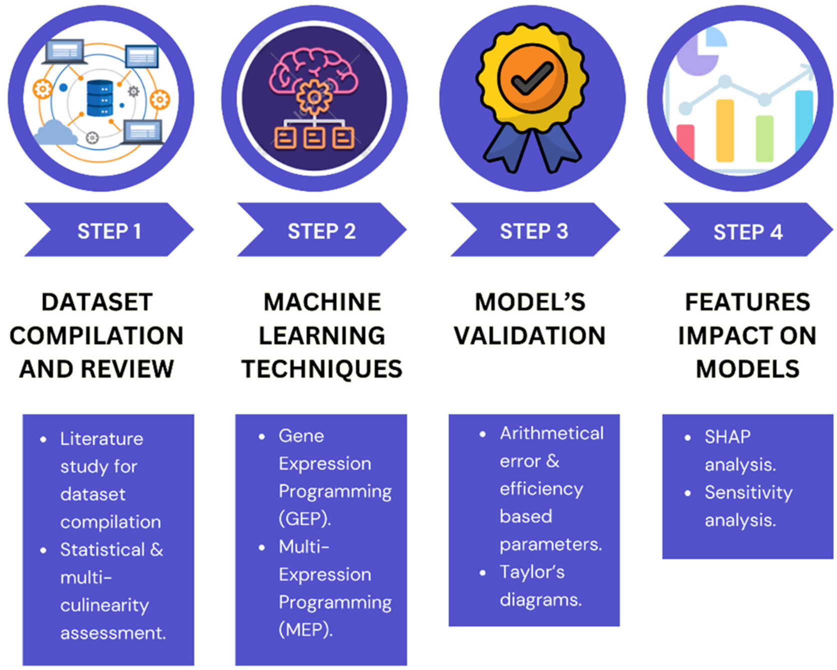

Figure 2: Four-step ML framework for predicting CS and TS of agro-waste concrete.

the average of the observed and predicted values, respectively. To assess the degree to which a simulation reliably reproduces or forecasts results, the correlation coefficient (R) is frequently employed. A higher R value reflects a strong linear association between the predicted and actual results, suggesting that the model reliably captures the underlying data trends [66]. The correlation coefficient (R) remains unaffected by the scaling of data, such as multiplication or division. However, the coefficient of determination (R^2) offers a more robust and informative measure of predictive accuracy. It quantifies how well the predicted values align with the actual data. An R^2 value closer to 1 indicates a highly dependable model with strong predictive capability and minimal deviation from observed outcomes [67,68]. The developed model exhibits enhanced predictive capability, evidenced by notable reductions in MAE and RMSE values. These error metrics consistently decrease as the model's accuracy improves, ideally approaching zero when discrepancies between actual and predicted values are minimized [69,70]. On the other hand, MAE has shown to be particularly reliable when applied to datasets characterized by continuous and smooth patterns, as confirmed through comprehensive analysis [71]. A reduction in prior error values corresponds to enhanced model performance, indicating greater predictive accuracy.

A Taylor diagram serves as an effective tool for evaluating a model's predictive performance. Among various statistical validation techniques, it stands out by visually summarizing how closely a model's output aligns with observed data. By comparing standard deviations, correlation coefficients, and centered root-mean-square differences relative to a reference point (the actual data), the diagram provides a comprehensive assessment of model accuracy and reliability [72,73]. The Taylor diagram graphically integrates three key statistical measures to assess model performance: standard deviation is shown along the axes, correlation coefficients are displayed as angular lines, and RMSE is represented by curved contours centered on the reference point (true values). This visual layout allows for a quick and effective comparison of models. The ideal model position is one that lies nearest to the reference point, indicating minimal error, high correlation, and strong predictive reliability [72].

3 Computational analysis and findings

3.1 CS models

3.1.1 GEP predictive model

To predict the CS of agro-waste-based concrete, the models employed ETs that embed mathematical structures influenced by genome distribution patterns and head length parameters. The construction of these ETs was primarily based on fundamental arithmetic operations, including multiplication, division, addition, subtraction, and exponentiation. These operations were strategically organized to construct subcomponents within the overall model. The GEP algorithm effectively transforms these structural elements into interpretable mathematical expressions that represent the predictive behavior of the model. Eq. (8) shows that by plugging in the feature values, these methods can predict the future CS of concrete made from agro-waste. Under ideal circumstances, the resultant model can beat it, but only if there is enough data. Figure 3(a) shows that the data are correctly matched because there is a solid black

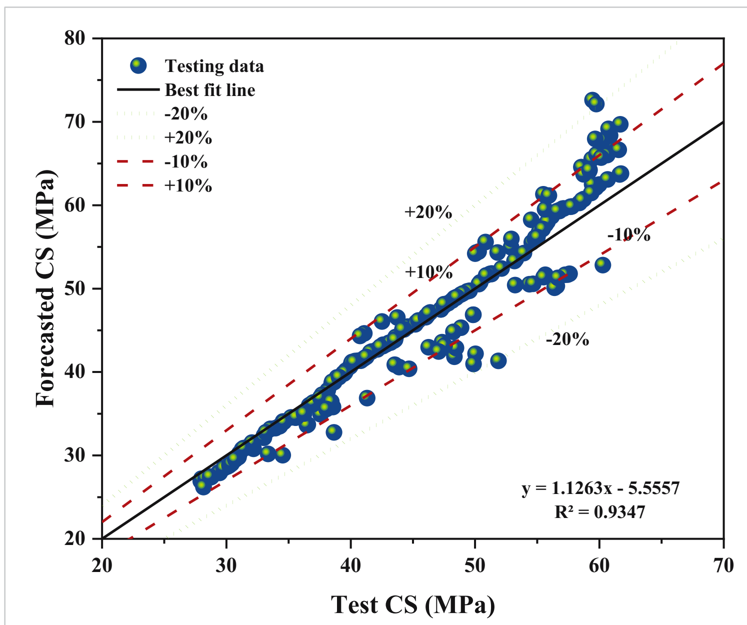

(a)

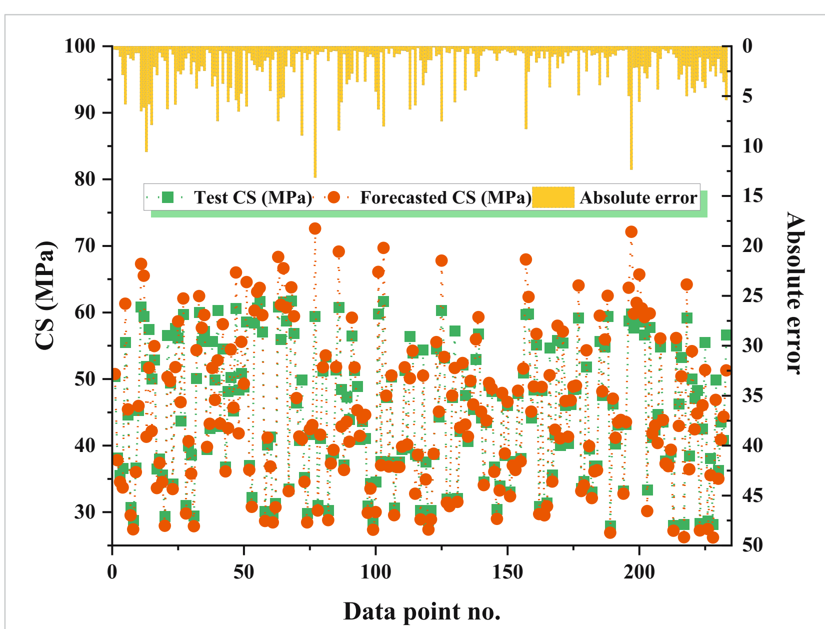

Figure 3: CS modeling with GEP: (a) Estimated *vs* observed CS relationship and (b) dataset-level error dispersion.

line there. The dotted green line shows a 20% change, whereas the dashed red line shows a 10% variance. The degree to which the experimental results match the projected CS values is shown by this graph. With a significant correlation shown by a R^2 value of 0.935, the GEP model successfully reproduced the reported CS values with little variation. Predicting CS using the GEP method was remarkably accurate; 99.1% of the values were within a 20% margin of error and 91.5% were within a 10% margin. Figure 3(b) shows the CS data *vs* the absolute error and may indicate a difference between the test values and the ones obtained by the GEP model. The findings demonstrated that the GEP-derived equation produced predictions that were closely aligned with the experimental outcomes, with absolute errors extending from 0.102 to 13.148 MPa. Figure 4 presents the error distribution, confirming the model's precision. Out of all predictions, 105 values exhibited errors below 1.0 MPa, while 98 fell within the 1.0–5.0 MPa range, and only 30 readings exceeded 5.0 MPa. High-magnitude errors were infrequent, highlighting the model's overall accuracy and reliability.

$$\begin{aligned}\mathrm{CS\ (MPa)} = {} & \mathrm{CCA} + \mathrm{POA} + \mathrm{RHA} + \mathrm{SBA} + \mathrm{WSA} \\ & + \mathrm{WCR} + (6.7040 \cdot \mathrm{WSA} \cdot \mathrm{RHA}) \\ & - (10.418 \cdot \mathrm{WCR}) + \left(\frac{5.1701}{\mathrm{WCR}}\right) + 13.3633 \\ & + 1.25 \cdot \log(\mathrm{CD} + 1) + 0.005 \cdot \mathrm{CD} \cdot \mathrm{WSA},\end{aligned} \tag{8}$$

where, CS: compressive strength, CCA: corn cob ash content, POA: palm oil ash content, SBA: sugarcane Bagasse ash content, RHA: rice husk ash content, WSA: wheat straw ash content, WCR: water-to-cementitious ratio, and CD: curing duration.

3.1.2 MEP predictive model

An analytical expression for predicting the CS of agro-waste-based concrete was derived using the results obtained from the MEP model. This model takes into consideration the cumulative impact of seven independent factors. The finalized mathematical representation generated through this modeling process is presented in Eq. (9).

$$\begin{aligned}\mathrm{CS(MPa)} = {} & \frac{2 \cdot \mathrm{WCR} \cdot (\mathrm{CD} + 1) \cdot \mathrm{WCR}^2 + (\mathrm{CD} + 1) \cdot \mathrm{WCR} \cdot (2 \cdot \mathrm{WCR}) \cdot \mathrm{POA}}{(2 \cdot \mathrm{WCR}) - 2 \cdot \log_{10}(\mathrm{CD})} \\ & + \frac{\mathrm{WCR} + (\mathrm{CD} + 1) \cdot \mathrm{WCR} + \mathrm{CCA} + \mathrm{WSA} + \mathrm{SBA} + \mathrm{RHA} \cdot 2 \cdot \log_{10}(\mathrm{CD})}{(2 \cdot \mathrm{WCR}) - 2 \cdot \log_{10}(\mathrm{CD})} \\ & + \frac{\mathrm{CD} + (\mathrm{CD} + 1) \cdot \mathrm{WCR}^2 \cdot \log_{10}(\mathrm{CD} + 1) - 1}{(2 \cdot \mathrm{WCR}) - 2 \cdot \log_{10}(\mathrm{CD})},\end{aligned} \tag{9}$$

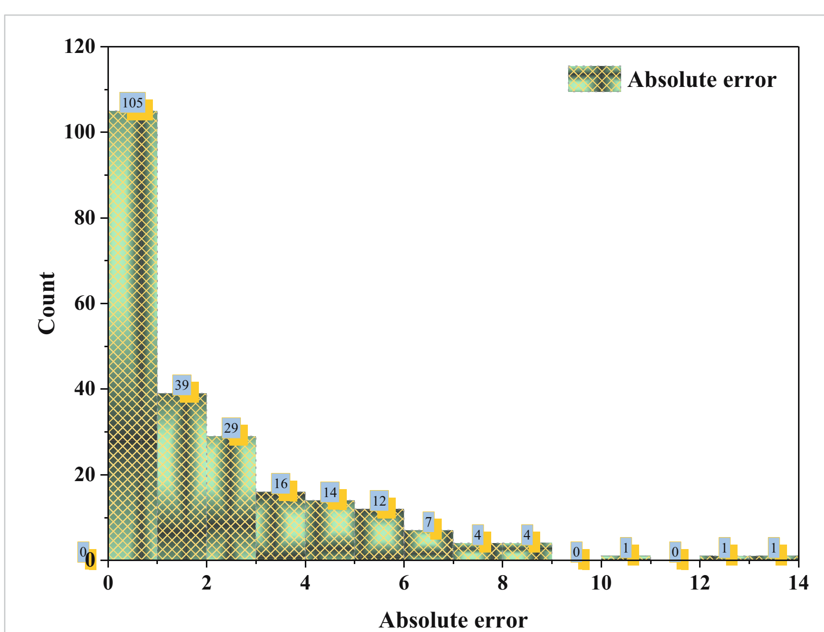

Figure 4: Residual error distribution of the CS-GEP model.

where, CS: compressive strength, CCA: corn cob ash content, RHA: rice husk ash content, POA: palm oil ash content, SBA: sugarcane Bagasse ash content, WSA: wheat straw ash content, WCR: water-to-cementitious ratio, and CD: curing duration.

Figure 5(a) provides evidence of the MEP model's resilience to simplification and proficiency; the figure also boasts an impressive R^2 value of 0.964. The CS model developed using MEP demonstrated greater reliability than the GEP model, as evidenced by its higher R^2 value. The solid

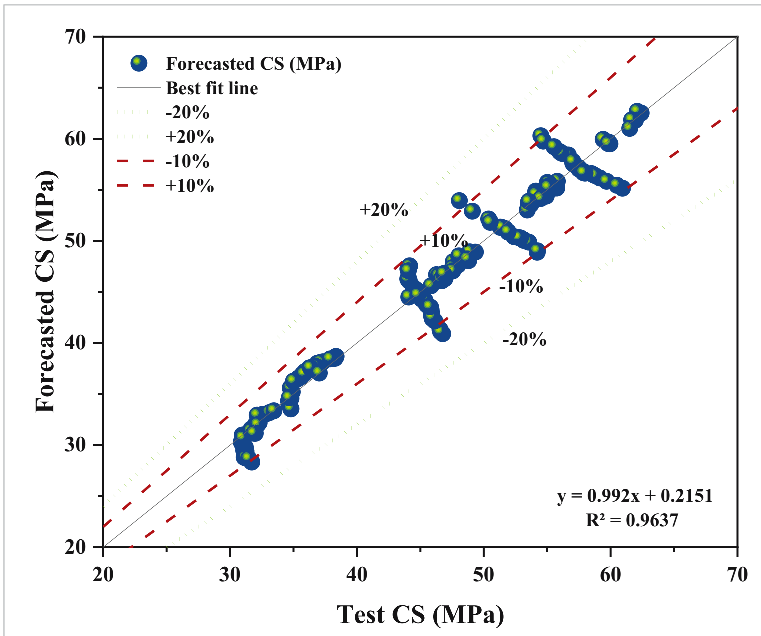

(a)

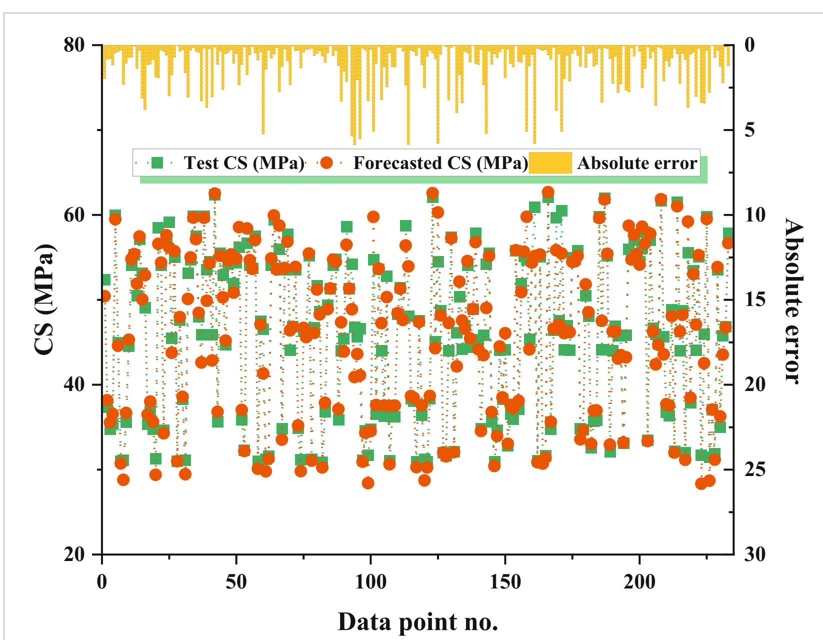

(b)

Figure 5: CS modeling with MEP: (a) Estimated *vs* observed CS relationship and (b) dataset-level error dispersion.

black line in Figure 5(a) displays a perfect one-to-one connection between the anticipated and actual values, whereas the dashed red and dotted green lines indicate variances of ±10 and ±20%, respectively. The predicted CS values from the MEP model align closely with the experimental data, indicating strong predictive performance and minimal deviation across the majority of observations. The MEP approach consistently produced precise CS calculations for agro-waste derived concrete. Its forecasts met or exceeded the 10% requirement in 97% of cases and the 20% barrier in 100% of cases, highlighting its remarkable accuracy.

Figure 5(b) illustrates the absolute error distribution between the measured and predicted CS values generated by the MEP model. This analysis highlights the model's ability to minimize prediction deviations, providing a clear depiction of how closely the estimated results align with experimental outcomes across the dataset. There is a wide variation in the MEP calculations, from 0.006 to 5.869 MPa, with an average error of 1.245 MPa. Nevertheless, the average inaccuracy is lower than 5.869 MPa; 137 of them are less than 1.0 MPa, 85 are between 1.0 and 5.0 MPa, and just 11 are greater than 5.0 MPa. Figure 6 shows a distribution plot comparing the MEP and GEP models. The MEP model has lower prediction variability, especially when outlier values are taken into consideration. This indicates a more stable and consistent performance of MEP in estimating CS. The GEP and MEP models both demonstrate great potential as accurate forecasters. In contrast, lowering the correlation coefficient and error standard deviations is achieved by utilizing the MEP equation. The MEP equation's popularity stems from its widespread use and adaptability.

3.2 TS models

3.2.1 GEP predictive model

The TS was computed by the models using ETs by utilizing mathematical correlations that emerged from the relationship between genome frequency and head size. Once the GEP method encodes the subexpression trees, it results in a complete algebraic equation as shown in Eq. (10), which can be utilized to estimate the TS of concrete incorporating agro-waste materials. When sufficient input data are provided, this model has the potential to perform even better than a theoretically ideal model. The solid black line in Figure 7(a) shows that the predicted and actual values are perfectly aligned. The red dashed line indicates a 10% deviation while the green dotted line represents a 20% variation. This figure highlights a strong correlation between the measured TS values and those predicted by the GEP model. The technique proved highly effective in estimating TS, achieving an R squared value of 0.946. Additionally, 82% of the predictions fell within a 10% error margin and 96% within a 20% range, demonstrating the

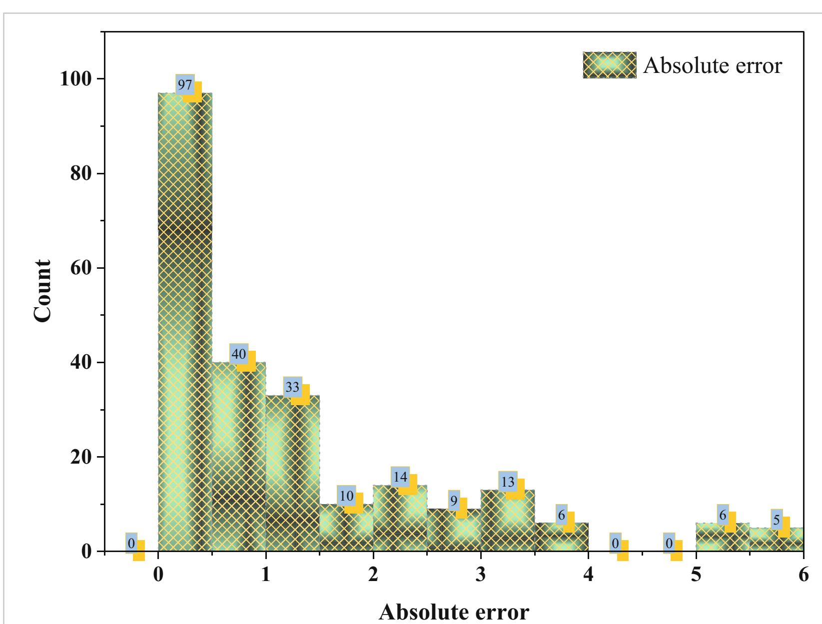

Figure 6: Residual error distribution of the CS-MEP model.

model's high level of precision. Figure 7(b) displays the absolute errors between the experimental and predicted values, revealing a close match between them. The model achieved an average absolute error of 0.253 MPa, with errors ranging from 0.002 to 2.519 MPa. Figure 8 shows that the error values have a dome-shaped distribution. In all, 189 of the erroneous values are between 0.2 and 0.5 MPa, with 123 of those being below 0.2 MPa and 21 beyond 0.5 MPa, according to the error distribution. It is rare for maximal error incidences to occur.

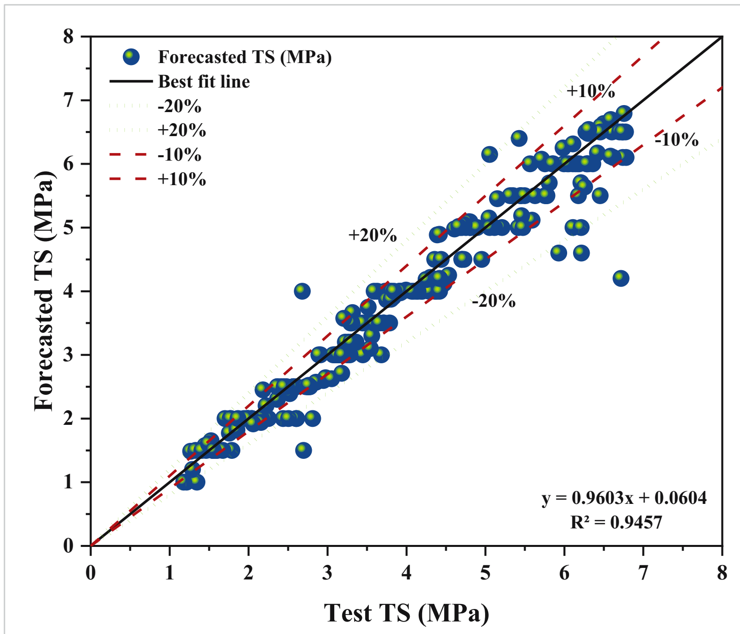

(a)

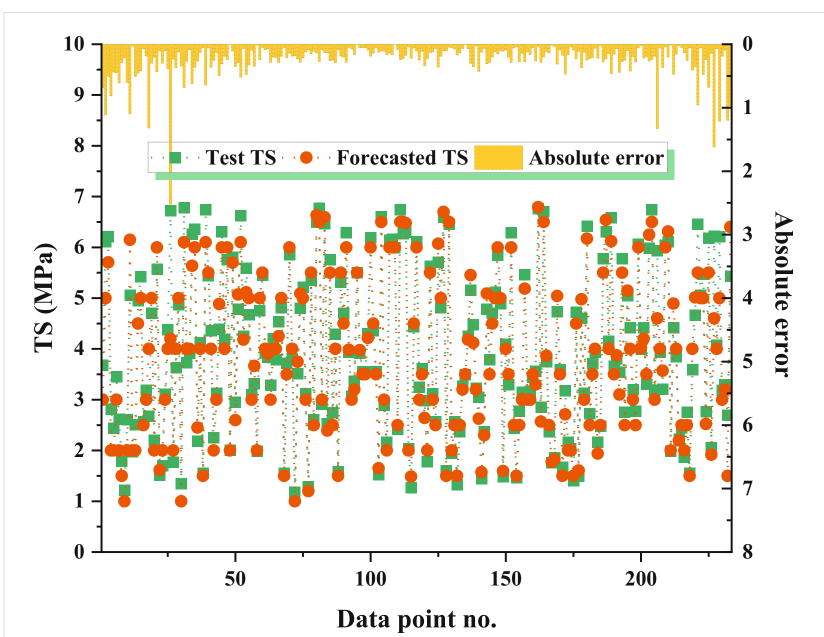

(b)

Figure 7: TS modeling with GEP: (a) Estimated *vs* observed TS relationship and (b) dataset-level error dispersion.

$$\begin{aligned}\text{TS (MPa)} = {} & [\log_{10}(\text{CD} + 7.6427) \\ & \cdot(\text{CCA} + 7.6427 + \text{SBA} - 3.1907) + \text{WCR}] \\ & \cdot(\text{RHA} + \text{CD} + \text{WCR}) \cdot \text{WCR} \\ & \cdot\left(\frac{\text{POA}}{((\text{WSA} - \text{WCR} + \text{CD})\cdot(\text{POA} + \text{WCR}) + \text{POA})}\right),\end{aligned} \tag{10}$$

where, TS: tensile strength, CCA: corn cob ash content, RHA: Rice husk ash content, POA: palm oil ash content, SBA: sugarcane Bagasse ash content, WSA: wheat straw ash content, WCR: water-to-cementitious tatio, and CD: curing duration.

3.2.2 MEP predictive model

An empirical formula was developed using the MEP results and the impacts of the seven independent components to determine the TS of agro-waste derived concrete. The final set of mathematical equations derived from modeling is shown in Eq. (11).

$$\begin{aligned}\text{TS (MPa)} = \log_{10}(&\text{RHA}^2 + (\text{SBA} + \text{WSA}) \cdot \text{CD} \\ & + (\text{SBA} + \text{WSA}) + (\text{SBA} - \text{CD}^2 + \text{CD}^3 \\ & + (\text{POA} + \text{CCA} - \text{CD})(\text{POA} + \text{CCA}))),\end{aligned} \tag{11}$$

where, TS: tensile strength, CCA: Corn cob ash content, RHA: rice husk ash content, POA: palm oil ash content, SBA: sugarcane Bagasse ash content, WSA: Wheat straw ash content, WCR: water-to-cementitious ratio, and CD: curing duration.

The MEP model demonstrated outstanding predictive capability for TS, as evidenced by its high *R* squared value of 0.961, shown in Figure 9(a). This strong correlation suggests that the model is robust and effectively captures the underlying complexity of the data without oversimplifying it. The MEP model for TS is more accurate than the GEP model, just as it is for CS. A perfect one-to-one correspondence between anticipated and actual values is shown by the solid black line in Figure 9(a), whereas lines representing 10 and 20% variances, respectively, are shown by the red and green lines. The predicted TS values closely followed the experimental results, showing strong consistency. Notably, 86% of the predicted values were within a 10% deviation and all predictions fell within the 20% range, confirming the exceptional accuracy and reliability of the MEP approach for modeling the TS of agro-waste-based concrete.

The MEP model simulation results are shown in Figure 9(b), with an emphasis on the absolute discrepancies between the actual and anticipated TS values. The data show that the model is very accurate, with an average error of only 0.239 MPa and individual errors ranging from 0.003 to 0.821 MPa. Further analysis in Figure 10 illustrates the distribution of these errors: 125 values fall below 0.2 MPa, 83 are between 0.2 and 0.5 MPa, and only 25 values exceed 0.5 MPa. Even when considering outlier values, the MEP model exhibits lower variability in results compared to the GEP model. Overall, both modeling techniques, MEP

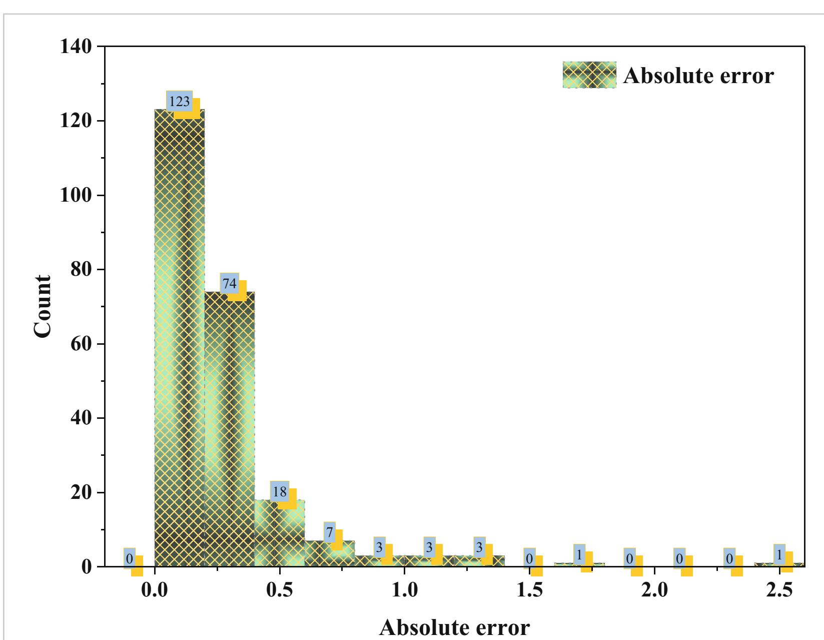

Figure 8: Residual error distribution of the TS-GEP model.

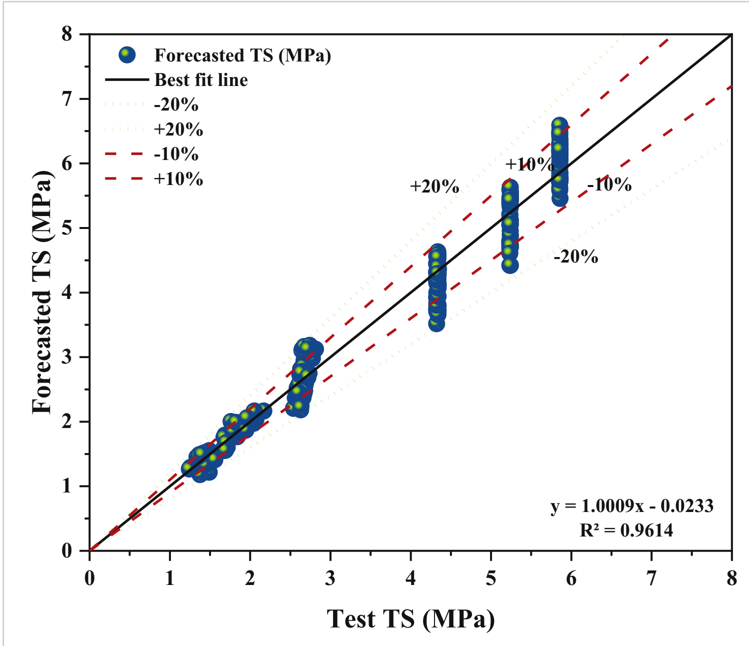

(a)

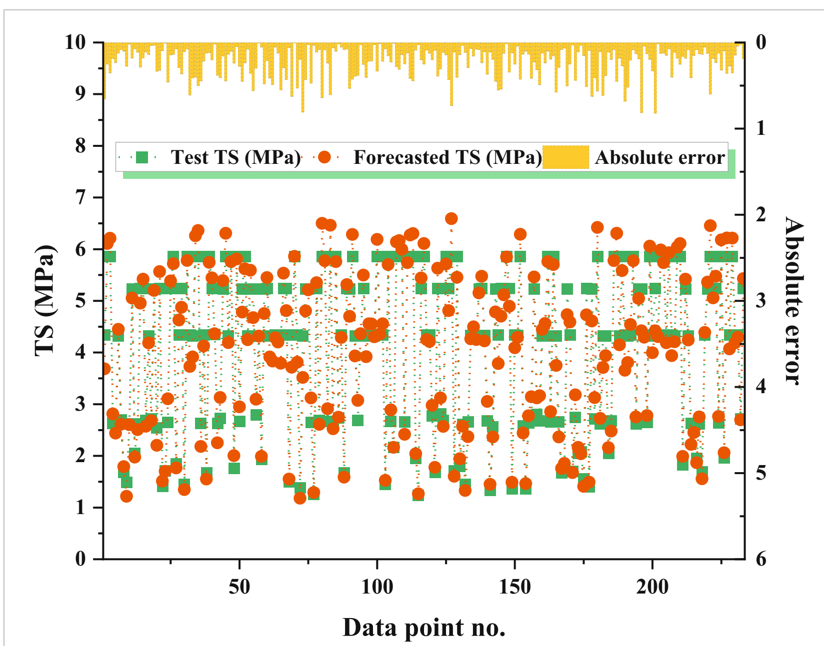

(b)

Figure 9: TS modeling with MEP: (a) Estimated *vs* observed TS relationship and (b) dataset-level error dispersion.

and GEP, have proven effective for predictive modeling, but MEP offers a distinct advantage. The reduced standard deviation in prediction errors and stronger correlation coefficients confirm that the MEP model delivers greater reliability and predictive accuracy than the GEP model.

3.3 Performance metrics and accuracy evaluation

Table 3 provides a comprehensive statistical comparison of GEP and MEP models for predicting the CS and TS of agro-

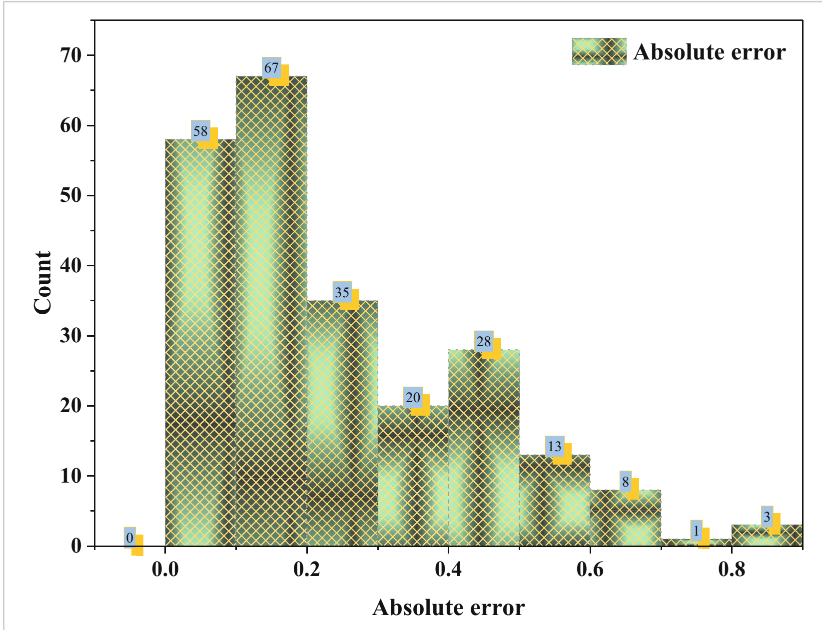

Figure 10: Residual error distribution of the TS-MEP model.

waste-based concrete. Across all key performance indicators including MAE, MAPE, RMSE, *R*, RSE, NSE, and RRMSE, the MEP model consistently outperforms GEP, demonstrating its superior predictive capability. For CS prediction, MEP shows notably lower error values such as MAE of 1.245 MPa, RMSE of 1.845 MPa, and MAPE of 2.70%, along with a higher correlation coefficient of 0.982 and improved NSE of 0.963. It also exhibits reduced RSE and RRMSE values, indicating closer alignment between predicted and actual outcomes. In TS prediction, MEP again performs slightly better with lower MAE of 0.239 MPa, RMSE of 0.301 MPa, and MAPE of 6.20%, accompanied by stronger correlation and efficiency values. These findings highlight the robustness of MEP in capturing the complex nonlinear relationships inherent in material behavior, making it a more accurate and dependable modeling approach than GEP for strength prediction in sustainable concrete studies. The Taylor diagram in Figure 11 offers a widespread association of all predictive models, demonstrating the close alignment of MEP models in forecasting the CS and TS of agro-waste derived concrete, while GEP models are relatively more divergent. Consistent with earlier research, the MEP model stands out as the best ML method for CS and TS prediction of agro-waste derived concrete, exhibiting the fewest outliers, most efficiency, and highest R^2 value. In conclusion, the analysis of error metrics and correlation efficiency statistics confirms that MEP is the more precise and efficient ML technique for predicting both CS and TS. The consistently lower prediction errors, stronger correlation coefficients, and superior efficiency metrics highlight its advantage over GEP, confirming its robustness and reliability for accurately predicting strength in material modeling applications.

Table 3: Comparative analysis of arithmetical indicators

Property	CS		TS	
	GEP	MEP	GEP	MEP
MAE (MPa)	2.198	1.245	0.254	0.239
MAPE (%)	4.50	2.70	6.80	6.20
NSE	0.895	0.963	0.942	0.960
R	0.967	0.982	0.972	0.981
RSE	0.344	0.262	0.384	0.342
RRMSE (MPa)	0.784	0.622	0.612	0.584
RMSE (MPa)	3.189	1.845	0.384	0.301

3.4 SHAP-based feature interpretation

The aim of this study is to explore the factors influencing the mechanical performance of concrete by analyzing its composition in detail. To understand both the overall and individual effects of input features, the SHAP tree explainer was utilized, which is widely adopted for interpreting model predictions globally. Figure 12 of the SHAP diagram shows that various input features affect agro-waste derived concrete's CS and TS. On the *X*-axis, the

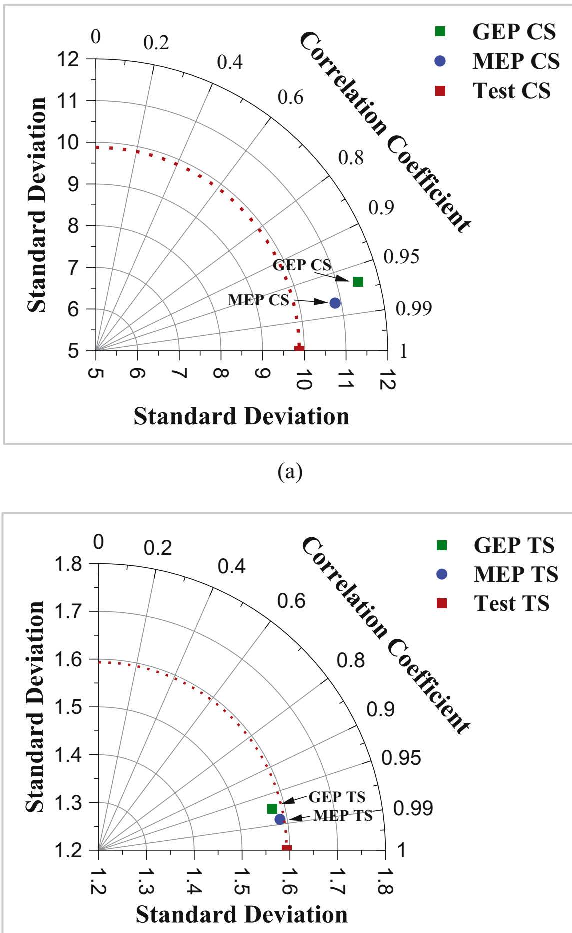

(a)

(b)

Figure 11: Taylor plots comparing predictive accuracy of models for (a) CS models and (b) TS models.

proportion of SHAP value associated with each raw material is shown, whereas the *Y*-axis represents the independent variables. As illustrated in the SHAP summary plot in Figure 12(a), the agro-waste content and the WCR emerge as the dominant factors influencing the prediction of CS in agro-waste-based concrete, whereas CD contributes the least. Higher agro-waste content generally contributes positively to CS due to its pozzolanic reactivity, which enhances the concrete matrix; however, an excessive amount may negatively affect strength, indicating a nonlinear relationship. In contrast, a lower WCR consistently leads to higher predicted CS, aligning with the fundamental principle that reduced water content enhances concrete density and strength by minimizing porosity. On the other hand, CD displays negligible variation in SHAP values, suggesting its limited influence within the dataset, possibly due to saturation in curing effect or a narrow range of CDs. A similar SHAP plot in Figure 12(b) for TS also reflects a comparable trend, where WCR and agro-waste remain dominant contributors. Specifically, low WCR values positively influence TS due to improved matrix cohesion, while moderate levels of agro-waste enhance TS *via* refined pore structure and better particle packing. However, excessive agro-waste still tends to reduce TS, highlighting the need for an optimal balance in mix design. CD again appears to have a minimal effect on TS prediction, reinforcing its secondary role in the model. The SHAP analysis provides engineers with a transparent understanding of how individual input variables, such as WCR, agro-waste content, and supplementary materials, influence CS and TS predictions. This interpretability allows engineers to identify optimal ranges of critical variables, diagnose poor-performing mix designs, and justify decisions with quantitative evidence.

3.5 Sensitivity analysis

This research looks into how different input characteristics affect the CS and TS predictions in agro-waste concrete. The input variables have a high correlation with the predicted outcome [74]. The sensitivity analysis in Figure 13 reveals that agro-waste is the most influential input, contributing 52% to the model's estimation of CS and TS. This highlights its critical role in enhancing mechanical performance, likely due to its pozzolanic and filler effects. WCR follows with a 38% impact, reflecting its importance in controlling hydration and porosity. CD has the least influence at 10%, suggesting that while it supports strength development, its effect is comparatively modest. Overall, the model is most sensitive to agro-waste and WCR, emphasizing their importance in optimizing strength outcomes. The results were greatly affected by the amount of input data points and the parameters used in the model. Keep in mind that the ML approach had varying effects on the study's results according to certain input variables, like the amounts of concrete mix. By focusing on the most sensitive parameters, engineers can design more efficient, reliable, and sustainable concrete mixes incorporating agro-waste materials. Eqs. (12) and (13) were used to determine the weights of the model's input parameters.

$$N_i = f_{\max}(x_i) - f_{\min}(x_i), \tag{12}$$

$$S_i = \frac{N_i}{\sum_{j-i}^{n} N_j}, \tag{13}$$

where the expression ($f_{\min}(x_i)$) describes the anticipated value with the lowest ith output, while the expression ($f_{\max}(x_i)$) represents the maximum.

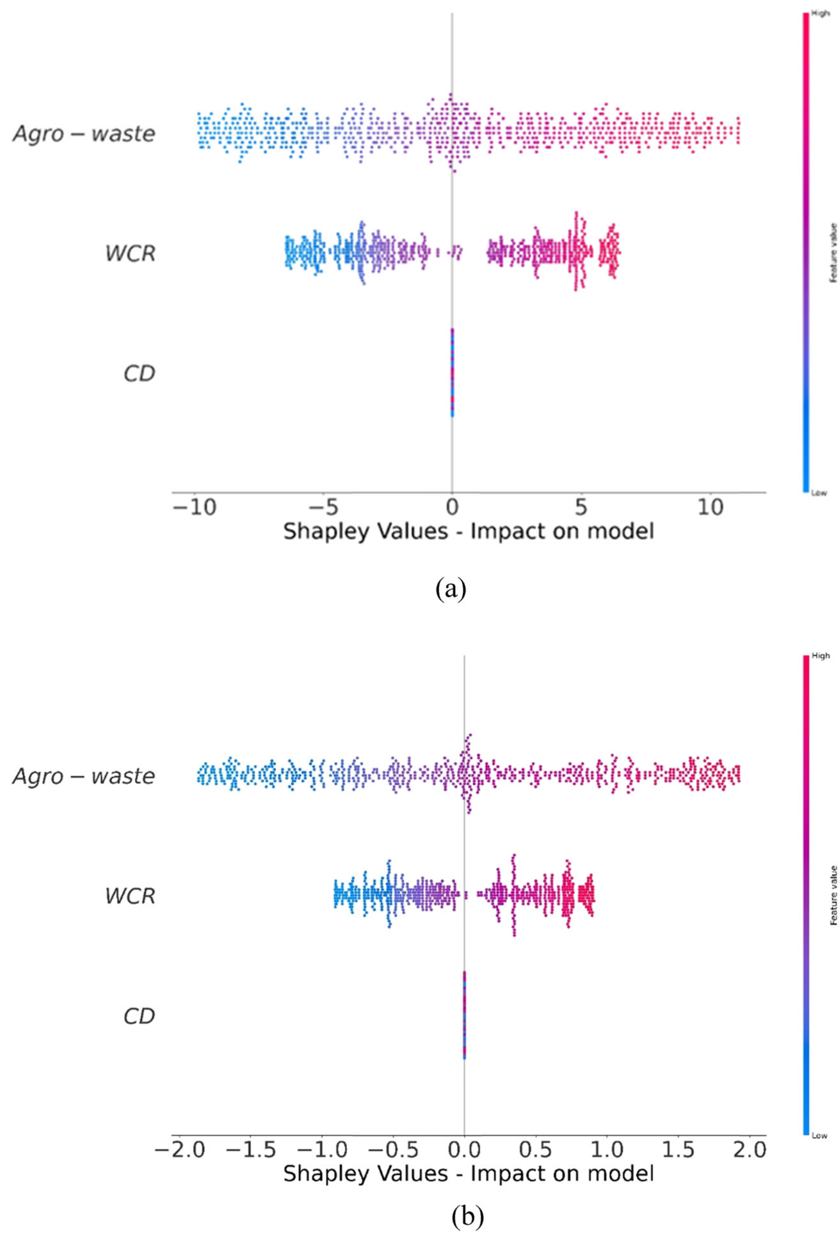

Figure 12: Influence of input variables: (a) CS predictions and (b) TS predictions.

4 Discussion

This study underscores the potential of integrating agricultural waste materials into concrete mix designs, presenting a promising pathway toward sustainable construction practices. Effective prediction of compressive and TSs of agro-waste-based concrete was achieved by the development and evaluation of two ML models, namely, GEP and MEP. A dataset of 700 literature-derived entries incorporating 7 input parameters revealed that MEP consistently outperformed GEP across all statistical metrics. Specifically, MEP achieved lower MAE and RMSE values along with higher coefficient of determination and Nash Sutcliffe efficiency scores, demonstrating improved accuracy and reliability in capturing complex nonlinear relationships. SHAP analysis confirmed the models' transparency by highlighting agro-waste content and WCR as the most influential features for both CS and TS predictions. In the case of CS, moderate levels of agro-waste improved strength through enhanced pozzolanic activity, while excessive replacement led to a decline. A lower WCR was linked with higher strength due to reduced porosity. For TS, a similar pattern emerged, where optimal agro-waste levels and lower WCR positively influenced tensile performance,

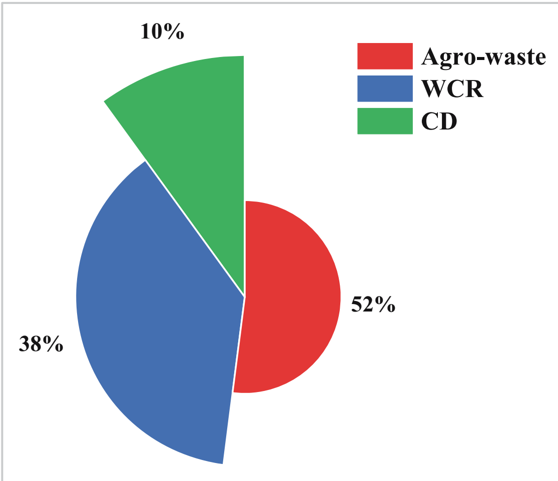

Figure 13: Proportional impact of inputs on prediction results.

further reinforcing the logical behavior of concrete composites. CD was shown to have a relatively lower impact on both strength parameters.

While the findings demonstrate the effectiveness of ML in optimizing sustainable concrete design, several limitations must be considered. ML models are inherently sensitive to the units and scales of input variables which can impact prediction accuracy if not properly standardized. Moreover, the dependence on a fixed set of input variables based on available literature data may reduce the models' adaptability to cases involving other influential factors not included in the dataset such as aggregate properties or environmental exposure conditions. Although SHAP and sensitivity analyses provide useful insights into feature contributions, their interpretations are statistical in nature and do not confirm causal relationships. The relatively low impact of CD observed in this study may be due to the narrow range of values in the dataset. Future work should include experimental validation, a wider range of input parameters and real-time data to strengthen the robustness, and practical utility of such models.

5 Conclusion

Using MEP and GEP for predictive modeling, this work examines the CS and TS of concrete integrating agro-waste materials. For training, testing, and validation purposes, a dataset was used that included 700 CS and TS values that were collected experimentally. Key conclusions that summarize the research outcomes are as follows.

- The GEP model had good success in predicting CS and TS agro-waste derived concrete, with R^2 values of 0.935 and 0.946, respectively. On the other hand, the MEP method proved to be more reliable in strength prediction, with R^2 values of 0.964 for CS and 0.961 for TS, demonstrating even greater accuracy and consistency.
- According to the error comparison, the MEP model shows improved accuracy and reliability in strength prediction compared to GEP, with CS's mean error dropping from 2.198 to 1.245 MPa and TS's from 0.254 to 0.239 MPa.
- The comparative results confirm that MEP consistently outperforms GEP in predicting CSs and TSs. For CS, MEP reduced RMSE from 3.189 to 1.845 MPa, MAE from 2.198 to 1.245 MPa, and improved NSE (from 0.895 to 0.963) and R (from 0.967 to 0.982). Similarly, for TS, MEP lowered RMSE from 0.384 to 0.301 MPa and enhanced NSE (from 0.942 to 0.960) and R (from 0.972 to 0.981). These improvements across all error and performance metrics demonstrate the superior accuracy and reliability of MEP in strength prediction.
- The SHAP analysis shows that WCR and agro-waste content are the most influential factors in predicting both CSs and TSs of agro-waste derived concrete. Lower WCR consistently enhances strength, while agro-waste improves strength up to an optimal level but reduces it when used excessively. CD has limited impact, indicating a secondary role in strength prediction.
- The sensitivity analysis confirms that agro-waste and WCR are the most impactful factors influencing the strength prediction of agro-waste derived concrete, contributing 52 and 38%, respectively. CD plays a lesser role at 10%. The model's performance also varies with the volume of mix and the chosen ML approach, underlining the importance of tailored input parameter selection.

Predicting features across various datasets is greatly assisted by the distinct mathematical frameworks of GEP and MEP. Decisions in material design can be made more efficiently with the help of these methods for evaluating, refining, and optimizing concrete mix proportions. By generating precise mathematical models, this study accelerates the assessment and enhancement of concrete mix formulations, empowering engineers and researchers to advance material development with greater speed and effectiveness.

Acknowledgments: This work was funded by the Deanship of Graduate Studies and Scientific Research at Jouf University under Grant No. (DGSSR-2025-02-01136).

Funding information: Deanship of Graduate Studies and Scientific Research at Jouf University under Grant No. (DGSSR-2025-02-01136).

Author contributions: F.A.: conceptualization, supervision, funding acquisition, project administration, formal analysis, writing, reviewing, and editing. R-U-D.N.: data acquisition, validation, resources, visualization, writing, reviewing, and editing. T.O.A.: investigation, conceptualization, resources, visualization, writing, reviewing, and editing. M.A.D.: methodology, validation, formal analysis, writing, reviewing, and editing. S.U.A.: software, methodology, validation, formal analysis, writing – original draft, reviewing, and editing. All authors have accepted responsibility for the entire content of this manuscript and approved its submission.

Conflict of interest: The authors state no conflict of interest.

Data availability statement: The datasets generated and/or analyzed during the current study are available from the corresponding author upon reasonable request.

References

[1] Ghosh, A. and G. D. Ransinchung. Application of machine learning algorithm to assess the efficacy of varying industrial wastes and curing methods on strength development of geopolymer concrete. *Construction and Building Materials*, Vol. 341, 2022, id. 127828.
[2] Belaïd, F. How does concrete and cement industry transformation contribute to mitigating climate change challenges? *Resources, Conservation & Recycling Advances*, Vol. 15, 2022, id. 200084.
[3] Ahmad, W., S. J. McCormack, and A. Byrne. Biocomposites for sustainable construction: A review of material properties, applications, research gaps, and contribution to circular economy. *Journal of Building Engineering*, Vol. 105, 2025, id. 112525.
[4] Andrew, R. M. Global CO_2 emissions from cement production, 1928–2018. *Earth System Science Data*, Vol. 11, 2019, pp. 1675–1710.
[5] Puertas, F., J. A. Suárez-Navarro, M. M. Alonso, and C. Gascó. NORM waste, cements, and concretes. A review. *Materiales de Construcción*, Vol. 71, No. 344, 2021, id. e259.
[6] Li, K., X. Wang, X. Wang, S. Tu, Y. Song, T. Shi, et al. A comprehensive benefit evaluation of recycled carbon fiber reinforced cement mortar based on combined weighting. *Construction and Building Materials*, Vol. 489, 2025, id. 142196.
[7] Elmagarhe, A., Q. Lu, M. Alharthai, M. Alamri, and A. Elnihum. Performance of porous asphalt mixtures containing recycled concrete aggregate and fly ash. *Materials*, Vol. 15, 2022, id. 6363.
[8] Schaubroeck, T., T. Gibon, E. Igos, and E. Benetto. Sustainability assessment of circular economy over time: Modelling of finite and variable loops & impact distribution among related products. *Resources, Conservation and Recycling*, Vol. 168, 2021, id. 105319.
[9] Jiang, Z., G. He, Y. Jiang, H. Zhao, Y. Duan, G. Yuan, et al. Synergistic preparation and properties of ceramic foams from wolframite tailings and high-borosilicate waste glass. *Construction and Building Materials*, Vol. 457, 2024, id. 139367.
[10] Shaaban, I. G., J. P. Rizzuto, A. El-Nemr, L. Bohan, H. Ahmed, and H. Tindyebwa. Mechanical properties and air permeability of concrete containing waste tires extracts. *Journal of Materials in Civil Engineering*, Vol. 33, 2021, id. 04020472.
[11] Nurruddin, M. F., H. Sani, B. S. Mohammed, and I. Shaaban. Methods of curing geopolymer concrete: A review. *International Journal of Advanced and Applied Sciences*, Vol. 5, 2018, pp. 31–36.
[12] Saif, M. S., A. S. Shanour, G. E. Abdelaziz, H. I. Elsayad, I. G. Shaaban, B. A. Tayeh, et al. Influence of blended powders on properties of ultra-high strength fibre reinforced self compacting concrete subjected to elevated temperatures. *Case Studies in Construction Materials*, Vol. 18, 2023, id. e01793.
[13] Khan, A. A., W. de Jong, P. J. Jansens, and H. Spliethoff. Biomass combustion in fluidized bed boilers: Potential problems and remedies. *Fuel Processing Technology*, Vol. 90, 2009, pp. 21–50.
[14] Liew, K. M., A. O. Sojobi, and L. W. Zhang. Green concrete: Prospects and challenges. *Construction and Building Materials*, Vol. 156, 2017, pp. 1063–1095.
[15] Khan, R., A. Jabbar, I. Ahmad, W. Khan, A. N. Khan, and J. Mirza. Reduction in environmental problems using rice-husk ash in concrete. *Construction and Building Materials*, Vol. 30, 2012, pp. 360–365.
[16] Hassan, A., T. Alomayri, M. F. Noaman, and C. Zhang. 3D printed concrete for sustainable construction: A review of mechanical properties and environmental impact. *Archives of Computational Methods in Engineering*, Vol. 32, 2025, pp. 1–31.
[17] Yang, L., Y. Gao, H. Chen, H. Jiao, M. Dong, T. A. Bier, et al. Three-dimensional concrete printing technology from a rheology perspective: a review. *Advances in Cement Research*, Vol. 36, 2024, pp. 567–586.
[18] Tangchirapat, W., T. Saeting, C. Jaturapitakkul, K. Kiattikomol, and A. Siripanichgorn. Use of waste ash from palm oil industry in concrete. *Waste Management*, Vol. 27, 2007, pp. 81–88.
[19] Mehta, P. K. Properties of blended cements made from rice husk ash. *Journal of the American Concrete Institute*, Vol. 74, 1977, pp. 440–442.
[20] Payá, J., J. Monzó, M. V. Borrachero, and E. Peris-Mora. Comparisons among magnetic and non-magnetic fly ash fractions: Strength development of cement-fly ash mortars. *Waste Management*, Vol. 16, 1996, pp. 119–124.
[21] Ismail, M. S. and A. M. Waliuddin. Effect of rice husk ash on high strength concrete. *Construction and Building Materials*, Vol. 10, 1996, pp. 521–526.
[22] Ahmad, W., V. S. S. C. S. Veeraghantla, and A. Byrne. Advancing sustainable concrete using biochar: Experimental and modelling study for mechanical strength evaluation. *Sustainability*, Vol. 17, 2025, id. 2516.
[23] Avci, O., O. Abdeljaber, S. Kiranyaz, M. Hussein, M. Gabbouj, and D. J. Inman. A review of vibration-based damage detection in civil structures: From traditional methods to Machine Learning and Deep Learning applications. *Mechanical Systems and Signal Processing*, Vol. 147, 2021, id. 107077.
[24] Ghahramani, Z. Probabilistic machine learning and artificial intelligence. *Nature*, Vol. 521, 2015, pp. 452–459.
[25] Long, X., M.-H. Mao, T.-X. Su, Y.-T. Su, and M.-K. Tian. Machine learning method to predict dynamic compressive response of concrete-like material at high strain rates. *Defence Technology*, Vol. 23, 2023, pp. 100–111.
[26] Stocker, T. *Climate change* 2013: the physical science basis: Working Group I contribution to the Fifth assessment report of the Intergovernmental Panel on Climate Change, Cambridge University Press, Cambridge, United Kingdom, 2014.
[27] Dietterich, T. G. *Ensemble methods in machine learning*, Springer, Berlin, Germany, 2000, pp. 1–15.

[28] Haenlein, M. and A. Kaplan. A brief history of artificial intelligence: On the past, present, and future of artificial intelligence. *California Management Review*, Vol. 61, 2019, pp. 5–14.

[29] Marani, A. and M. L. Nehdi. Machine learning prediction of compressive strength for phase change materials integrated cementitious composites. *Construction and Building Materials*, Vol. 265, 2020, id. 120286.

[30] Ahmad, A., W. Ahmad, F. Aslam, and P. Joyklad. Compressive strength prediction of fly ash-based geopolymer concrete via advanced machine learning techniques. *Case Studies in Construction Materials*, Vol. 16, 2022, id. e00840.

[31] Peng, Y. and C. Unluer. Analyzing the mechanical performance of fly ash-based geopolymer concrete with different machine learning techniques. *Construction and Building Materials*, Vol. 316, 2022, id. 125785.

[32] Timur Cihan, M. Prediction of concrete compressive strength and slump by machine learning methods. *Advances in Civil Engineering*, Vol. 2019, 2019, pp. 1–11.

[33] Tamimi, A. K., J. A. Abdalla, and Z. I. Sakka. Prediction of long term chloride diffusion of concrete in harsh environment. *Construction and Building Materials*, Vol. 22, 2008, pp. 829–836.

[34] Zhang, W., S. Zhang, J. Wei, and Y. Huang. Flexural behavior of SFRC-NC composite beams: An experimental and numerical analytical study. *Structures*, Vol. 60, 2024, id. 105823.

[35] Zhang, W., X. Liu, Y. Huang, and M.-N. Tong. Reliability-based analysis of the flexural strength of concrete beams reinforced with hybrid BFRP and steel rebars. *Archives of Civil and Mechanical Engineering*, Vol. 22, 2022, id. 171.

[36] Nazar, S., J. Yang, A. Ahmad, and S. F. A. Shah. Comparative study of evolutionary artificial intelligence approaches to predict the rheological properties of fresh concrete. *Materials Today Communications*, Vol. 32, 2022, id. 103964.

[37] Song, H., A. Ahmad, F. Farooq, K. A. Ostrowski, M. Maślak, S. Czarnecki, et al. Predicting the compressive strength of concrete with fly ash admixture using machine learning algorithms. *Construction and Building Materials*, Vol. 308, 2021, id. 125021.

[38] Moein, M. M., A. Saradar, K. Rahmati, S. H. G. Mousavinejad, J. Bristow, V. Aramali, et al. Predictive models for concrete properties using machine learning and deep learning approaches: A review. *Journal of Building Engineering*, Vol. 63, 2022, id. 105444.

[39] Niu, Y., W. Wang, Y. Su, F. Jia, and X. Long. Plastic damage prediction of concrete under compression based on deep learning. *Acta Mechanica*, Vol. 235, 2024, pp. 255–266.

[40] Abbas, A., G. Fathifazl, O. B. Isgor, A. G. Razaqpur, B. Fournier, and S. Foo. *Environmental benefits of green concrete*, IEEE, New York, USA, 2006, pp. 1–8.

[41] Baigh, T. A. and F. Nanzeeba. *Integration and mechanical characterization of PALF and jute fibre in epoxy polymer to fabricate structural hybrid biocomposites*, Islamic University of Technology (Doctoral Dissertation), Gazipur, Bangladesh, 2023.

[42] Meyer, C. The greening of the concrete industry. *Cement and Concrete Composites*, Vol. 31, 2009, pp. 601–605.

[43] Siddique, R. *Waste materials and by-products in concrete*, Springer Science & Business Media, Berlin, Germany, 2007.

[44] Amran, M., R. Fediuk, G. Murali, N. Vatin, M. Karelina, T. Ozbakkaloglu, et al. Rice husk ash-based concrete composites: A critical review of their properties and applications. *Crystals*, Vol. 11, 2021, id. 168.

[45] Sobuz, M. H. R., S. D. Datta, J. A. Jabin, F. S. Aditto, N. M. S. Hasan, M. Hasan, et al. Assessing the influence of sugarcane bagasse ash for the production of eco-friendly concrete: Experimental and machine learning approaches. *Case Studies in Construction Materials*, Vol. 20, 2024, id. e02839.

[46] Naik, T. R. Sustainability of the cement and concrete industries. In *Sustainable construction materials and technologies*, CRC Press, Boca Raton, Florida, USA, 2020, pp. 19–25.

[47] Chandra Paul, S., P. B. K. Mbewe, S. Y. Kong, and B. Šavija. Agricultural solid waste as source of supplementary cementitious materials in developing countries. *Materials*, Vol. 12, 2019, id. 1112.

[48] Shukla, A., C. K. Singh, and A. K. Sharma. Study of the properties of concrete by partial replacement of ordinary Portland cement by rice husk ash. *International Journal of Earth Sciences and Engineering*, Vol. 4, No. 6, 2011, pp. 965–968.

[49] Meddah, M. S., P. T. Ramesh, and M. Sekar. Properties of Sugarcane Bagasse Ash Concrete Modified with Bacterial Treatment. *ACI Materials Journal*, Vol. 119, 2022, pp. 187–196.

[50] He, J., S. Kawasaki, and V. Achal. The utilization of agricultural waste as agro-cement in concrete: A review. *Sustainability*, Vol. 12, 2020, id. 6971.

[51] Nwakaire, C. M., C. H. Aginam, and C. A. Chidolue. Prospects of partial substitution of cement with rice husk ash for road concrete works. *Journal of Architectural Environment & Structural Engineering Research*, Vol. 3, 2020, pp. 17–25.

[52] Cordeiro, G. C., R. D. Toledo Filho, and E. de Moraes Rego Fairbairn. Use of ultrafine rice husk ash with high-carbon content as pozzolan in high performance concrete. *Materials and Structures*, Vol. 42, 2009, pp. 983–992.

[53] Oliko, C., C. K. Kabubo, and J. N. Mwero. Rice straw and eggshell ash as partial replacements of cement in concrete. *Engineering, Technology & Applied Science Research*, Vol. 10, 2020, pp. 6481–6487.

[54] Jain, V., B. Jain, and G. Sancheti. Influence of Rice Husk Ash (RHA) on the workability of concrete. *Earth and Environmental Science*, Vol. 796, 2021, id. 012073.

[55] Ahmad, W., A. Ahmad, K. A. Ostrowski, F. Aslam, P. Joyklad, and P. Zajdel. Sustainable approach of using sugarcane bagasse ash in cement-based composites: A systematic review. *Case Studies in Construction Materials*, Vol. 15, 2021, id. e00698.

[56] Jittin, V., S. N. Minnu, and A. Bahurudeen. Potential of sugarcane bagasse ash as supplementary cementitious material and comparison with currently used rice husk ash. *Construction and Building Materials*, Vol. 273, 2021, id. 121679.

[57] Zerbino, R., G. Giaccio, and G. C. Isaia. Concrete incorporating rice-husk ash without processing. *Construction and Building Materials*, Vol. 25, 2011, pp. 371–378.

[58] Zhang, M.-h, R. Lastra, and V. M. Malhotra. Rice-husk ash paste and concrete: some aspects of hydration and the microstructure of the interfacial zone between the aggregate and paste. *Cement and Concrete Research*, Vol. 26, 1996, pp. 963–977.

[59] Athira, G. and A. Bahurudeen. Rheological properties of cement paste blended with sugarcane bagasse ash and rice straw ash. *Construction and Building Materials*, Vol. 332, 2022, id. 127377.

[60] Lee, B. C. and D. M. Brooks. Accurate and efficient regression modeling for microarchitectural performance and power prediction. *ACM SIGOPS Operating Systems Review*, Vol. 40, 2006, pp. 185–194.

[61] Iqbal, M. F., Q.-f Liu, I. Azim, X. Zhu, J. Yang, M. F. Javed, et al. Prediction of mechanical properties of green concrete incorporating waste foundry sand based on gene expression

programming. *Journal of Hazardous Materials*, Vol. 384, 2020, id. 121322.
[62] Mohammadzadeh S, D., S.-F. Kazemi, A. Mosavi, E. Nasseralshariati, and J. H. M. Tah. Prediction of compression index of fine-grained soils using a gene expression programming model. *Infrastructures*, Vol. 4, 2019, id. 26.
[63] Shahin, M. A. *Genetic programming for modelling of geotechnical engineering systems*, Springer International, Cham, Switzerland, 2015.
[64] Çanakcı, H., A. Baykasoğlu, and H. Güllü. Prediction of compressive and tensile strength of Gaziantep basalts via neural networks and gene expression programming. *Neural Computing and Applications*, Vol. 18, 2009, pp. 1031–1041.
[65] Alade, I. O., M. A. Abd Rahman, and T. A. Saleh. Predicting the specific heat capacity of alumina/ethylene glycol nanofluids using support vector regression model optimized with Bayesian algorithm. *Solar Energy*, Vol. 183, 2019, pp. 74–82.
[66] Alade, I. O., A. Bagudu, T. A. Oyehan, M. A. Abd Rahman, T. A. Saleh, and S. O. Olatunji. Estimating the refractive index of oxygenated and deoxygenated hemoglobin using genetic algorithm–support vector regression model. *Computer Methods and Programs in Biomedicine*, Vol. 163, 2018, pp. 135–142.
[67] Zhang, W., R. Zhang, C. Wu, A. T. C. Goh, S. Lacasse, Z. Liu, et al. State-of-the-art review of soft computing applications in underground excavations. *Geoscience Frontiers*, Vol. 11, 2020, pp. 1095–1106.
[68] Alavi, A. H., A. H. Gandomi, H. C. Nejad, A. Mollahasani, and A. Rashed. Design equations for prediction of pressuremeter soil deformation moduli utilizing expression programming systems. *Neural Computing and Applications*, Vol. 23, 2013, pp. 1771–1786.
[69] Kisi, O., J. Shiri, and M. Tombul. Modeling rainfall-runoff process using soft computing techniques. *Computers & Geosciences*, Vol. 51, 2013, pp. 108–117.
[70] Alade, I. O., M. A. Abd Rahman, and T. A. Saleh. Modeling and prediction of the specific heat capacity of Al_2O_3/water nanofluids using hybrid genetic algorithm/support vector regression model. *Nano-Structures & Nano-Objects*, Vol. 17, 2019, pp. 103–111.
[71] Shahin, M. A. Use of evolutionary computing for modelling some complex problems in geotechnical engineering. *Geomechanics and Geoengineering*, Vol. 10, 2015, pp. 109–125.
[72] Band, S. S., E. Heggy, S. M. Bateni, H. Karami, M. Rabiee, S. Samadianfard, et al. Groundwater level prediction in arid areas using wavelet analysis and Gaussian process regression. *Engineering Applications of Computational Fluid Mechanics*, Vol. 15, 2021, pp. 1147–1158.
[73] Taylor, K. E. Summarizing multiple aspects of model performance in a single diagram. *Journal of Geophysical Research: Atmospheres*, Vol. 106, 2001, pp. 7183–7192.
[74] Ahmad, A., K. A.Ostrowski, M.Maślak, F.Farooq, I.Mehmood, and A.Nafees. Comparative study of supervised machine learning algorithms for predicting the compressive strength of concrete at high temperature. *Materials*, Vol. 14, 2021, id. 4222.